Short Communication

# Neuroradiological findings in three cases of pontocerebellar hypoplasia type 9 due to *AMPD2* mutation: typical MRI appearances and pearls for differential diagnosis

**Elisa Scola[1], Mario Ganau[2], Robert Robinson[3], Maureen Cleary[4], Laurens J. L. De Cocker[5], Kshitij Mankad[6], Fabio Triulzi[1,7], Felice D'Arco[6]**

[1]Department of Neuroradiology, Fondazione IRCCS Ca' Granda Ospedale Maggiore Policlinico, Milan, Italy; [2]Department of Neurosurgery, Oxford University Hospitals NHS Foundation Trust, Oxford, UK; [3]Department of Neurology, [4]Department of Metabolic Medicine, Great Ormond Street Hospital NHS Foundation Trust, London, UK; [5]Department of Radiology, AZ Maria Middelares, Ghent, Belgium; [6]Department of Radiology, Great Ormond Street Hospital NHS Foundation Trust, London, UK; [7]Università degli Studi Milano, Milan, Italy

*Correspondence to:* Dr. Elisa Scola. Neuroradiology Unit, Fondazione IRCCS Ca'Granda Ospedale Maggiore Policlinico, Via Francesco Sforza 35, Milan 20122, Italy. Email: elisa.scola@policlinico.mi.it.

**Abstract:** Pontocerebellar hypoplasia type 9 (PCH9) is a rare autosomal recessive neurodegenerative disorder with prenatal onset caused by mutations in adenosine monophosphate deaminase 2 (*AMPD2*). PCH9 patients demonstrate severe neurodevelopmental delay with early onset and typical magnetic resonance imaging (MRI) findings consisting in: pontine hypoplasia or atrophy with dragonfly cerebellar atrophy appearance on coronal images, reduction in size of the pons and middle cerebellar peduncles, abnormal midbrain describing a figure of "8" on axial images, diffuse loss of cerebral white matter with striking periventricular leukomalacia (PVL), and absence or extreme thinning of the corpus callosum. A review of the literature on PCH9 shows that the MRI phenotype observed in the series herein presented is similar to the eleven cases of PCH9 previously reported. Finally, the main radiological elements which differentiate this diagnosis from other PCH subtypes are described.

**Keywords:** Pontocerebellar hypoplasia type 9 (PCH9); magnetic resonance imaging (MRI); *AMPD2* mutations; pediatric posterior fossa

Submitted May 30, 2019. Accepted for publication Aug 12, 2019.
doi: 10.21037/qims.2019.08.12
**View this article at:** http://dx.doi.org/10.21037/qims.2019.08.12

## Introduction

Pontocerebellar hypoplasia type 9 (PCH9) is a rare autosomal recessive neurodegenerative disorder with prenatal onset caused by mutations in the adenosine monophosphate deaminase 2 (*AMPD2*) gene (OMIM# 615809) which is necessary for guanine nucleotide biosynthesis, protein translation and neurogenesis (1). Affected patients present with neurodevelopmental delay, truncal hypotonia, neonatal clonus and facial dysmorphism. Cerebral visual impairment, swallowing difficulties, spasticity and hypereflexia are always present (2-5). Neuroimaging features have been recently described and include pontine hypoplasia/atrophy, a figure of "8" of the midbrain on axial plane, cerebellar atrophy affecting the hemispheres more than the vermis, marked periventricular leukomalacia (PVL) and hypoplasia/absence of the corpus callosum (1-5).

The aim of this article is to report the neuroradiological findings in three new cases of PCH9 with *AMPD2* mutation and provide a review of the literature on radiological appearances of other pontocerebellar hypoplasias (PCHs) with a specific focus on their differential diagnosis. With

 

this short report, we intend to raise awareness among radiologists on the fairly typical neuroradiological findings in PCH9 and allow prompt diagnosis of this rare condition.

## Case series

### *Clinical presentation and evolution*

**Patient 1**

A 7-year-old female with a homozygous pathogenic variant of *AMPD2* (both parents were heterozygous variants). She presented with severe global developmental delay and arrest of development in the first years of life. Subsequently, she developed spasticity in all four limbs, visual impairment, feeding difficulties that required gastrostomy, subluxation of hips and bilateral talipes.

**Patient 2**

Sister of patient 1; she presented at 4 years of age with strikingly similar symptoms and signs to her sister (developmental arrest, congenital talipes and spasticity).

**Patient 3**

A 2-year-old female heterozygous for a non-sense pathogenic variant of *AMPD2* and for a missense variant in the same gene. She presented at 4 months of age with microcephaly, an evolving spastic-dystonic movement disorder, truncal hypotonia, intractable epilepsy and abnormal visual behavior.

### *Magnetic resonance imaging (MRI) findings*

All patients underwent MRI of the brain: patient 1 at 9 months of age, patient 2 at 7 months of age and patient 3 at 18 months of age. MRI findings were very similar in all individuals: the cerebellum and the pons were hypoplastic with a "dragonfly" appearance (i.e., marked atrophy of the hemispheres and a relative sparing of the vermis), the midbrain in axial views had a figure of "8" appearance, the corpus callosum was severely hypoplastic and there were diffuse PVL and global reduction of the white matter bulk (resembling the pattern of PVL described in preterm infant but more extensive). Moreover, the basal ganglia and thalami were severely hypoplastic, in particular the globi pallidi.

*Figure 1* shows the constellation of findings in the subjects.

Informed consent was obtained from the parents of all patients included in the study.

## Discussion

PCH9 is a rare autosomal recessive neurodegenerative disorders with prenatal onset presenting with severe neurodevelopmental delay, microcephaly, axonal neuropathy and epilepsy (1,2). We describe 3 patients with strikingly similar constellation of brain findings. Abnormalities on MRI were also comparable to those previously described in literature and include a characteristic combination of "dragonfly" PCH, a figure of "8" appearance of midbrain on axial plane, progressive microcephaly and marked global reduction of the cerebral white matter in keeping with PVL. As a consequence of the marked reduction of the cerebral white matter bulk, the corpus callosum was extremely thinned or absent (2-5). The figure of "8" shape of the midbrain probably results from a marked thinning of cortico-spinal tract, as shown by a previous DTI study (3).

Our cases and the scarce literature available confirm that the diagnosis of *AMPD2* mutation/PCH9 can be done based on pathognomonic brain MRI findings.

Akizu *et al.* (4) reported 5 patients with a similar structural brain anomaly characterized by hypoplasia/atrophy of cerebellum and flattening of the ventral part of pons but also atrophy of cerebral cortex and hypoplasia of corpus callosum. In the cerebellum, relative sparing of the vermis, gave a characteristic dragonfly appearance. Marsh *et al.* (2) described 5 affected siblings with *AMPD2* mutation all showing the same neuroradiological findings but with complete absence of the corpus callosum. One patient in this series had both prenatal (at 30 weeks gestation) and postnatal MRI scans suggesting a fetal onset with progressive loss of volume overtime. Interestingly our cases show preservation of the cingulate gyrus. Thus, we think that, given the embryological link between cingulate gyrus and corpus callosum, and the progressive, rather than absent, PVL in all PCH9, the callosum may be just extremely thinned in these patients.

To date, 17 variants have been associated with PCH9: ten missense, three nonsense, three frameshift and one splice site variant (1). The PCH9-associated *AMPD2* pathogenic variants mainly localize within the catalytic *AMPD2* domain (2,4), this gene encodes one of three known AMP deaminase homologs which is necessary for guanine nucleotide biosynthesis, protein translation and neurogenesis (4).

 

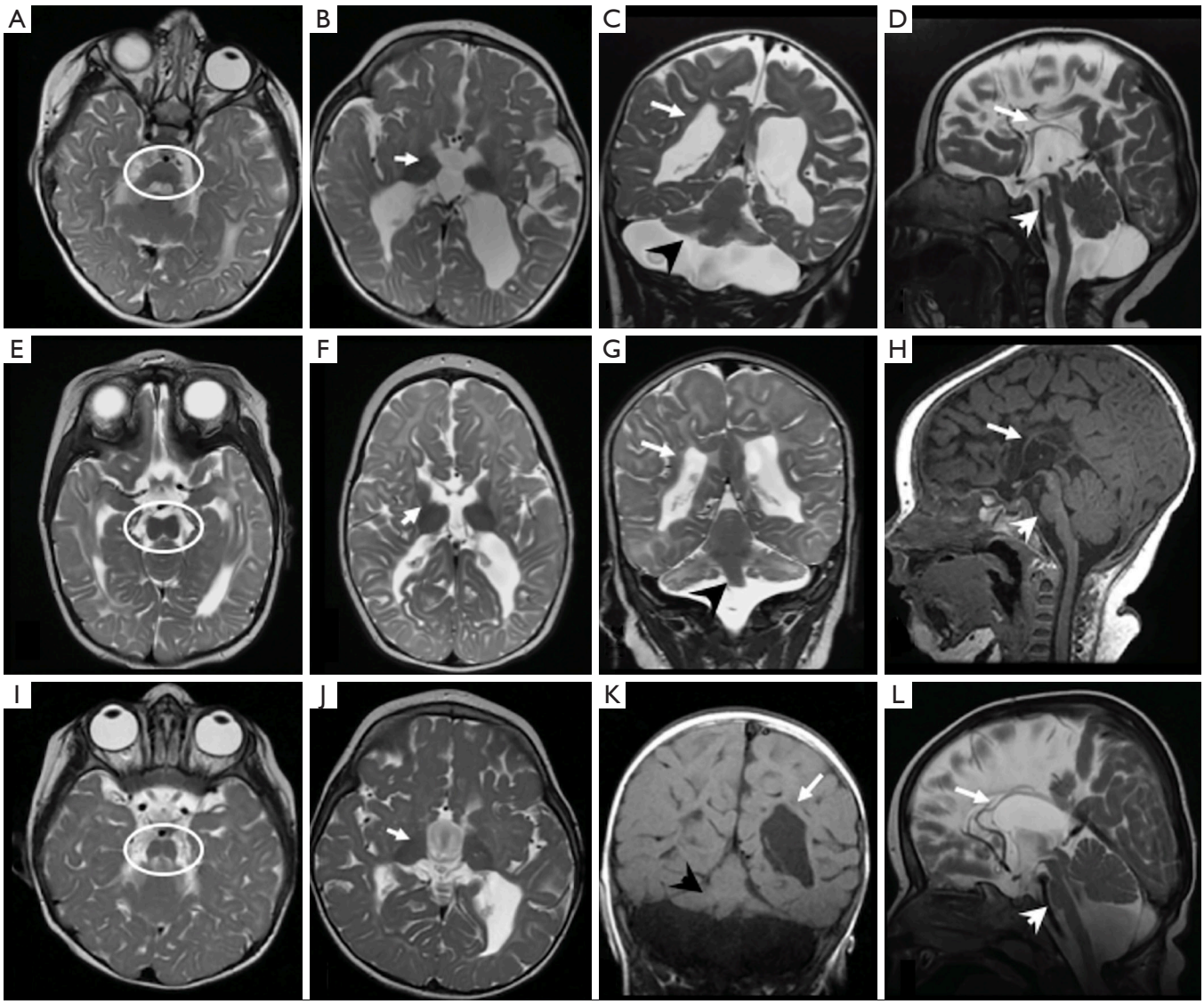


**Figure 1** Brain MRIs from patient 1 (A-D), patient 2 (E-H) and patient 3 (I-L) with pontocerebellar hypoplasia 9. Axial T2-weighted images (A,B,E,F,I,J) show characteristic "figure of 8" midbrain appearance (white ovals) and small basal ganglia and thalami (white arrows). Coronal images (C,G,K) reveal hypoplasia/atrophy of the cerebellar hemispheres with relative sparing of the vermis (dragonfly appearance-black arrowheads), periventricular leukomalacia and enlarged lateral ventricles (white arrows). Sagittal T1 and T2-weighted images (D,H,L) show small pons (white arrowheads) and extreme thinning of corpus callosum (white arrows). MRI, magnetic resonance imaging.

## Radiological differential diagnosis with other PCH subtypes (*Figure 2*): a pattern-recognition approach

A total of 11 different subtypes of PCH have been described according to their genetic basis; they show a remarkable clinical variability and differ also in terms of neuroimaging findings. As a general rule, pontocerebellar involvement is a consistent feature on MRI, even if severe cerebellar symptoms are seldom described.

### *"Dragonfly" vs. "Butterfly" cerebellum*

Based on coronal images, the cerebellar appearances can be distinguished into different groups: a dragonfly type, with relatively preserved vermis and atrophic cerebellar

 

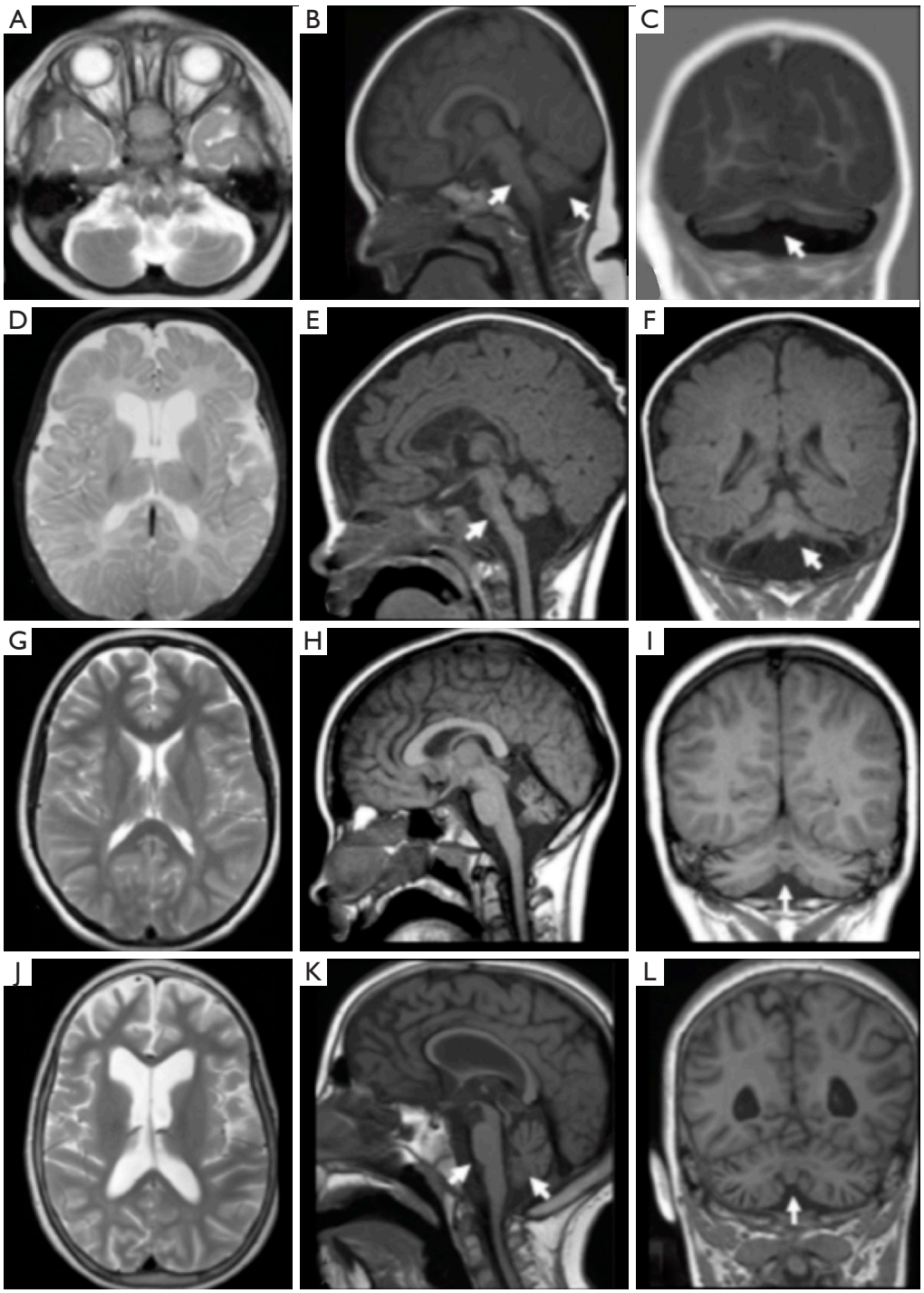


**Figure 2** (A-C) MR T2 axial, T1 sagittal and coronal images of a 11-year-old patient with *CASK4* mutation showing pontocerebellar hypoplasia with typical butterfly appearance on coronal images (white arrows). Note normal appearing corpus callosum; (D,E) MR T2 axial, T1 sagittal and coronal images of a 3-month-old patient with pontocerebellar hypoplasia 2A (*TSEN54* mutation) showing pontocerebellar hypoplasia with dragonfly appearance on coronal images (white arrows); (G-I) MR T2 axial, T1 sagittal and coronal images of a 3-month-old patient with pontocerebellar hypoplasia 1B (*EXOSC3* mutation) showing cerebellar atrophy with butterfly appearance on coronal images (white arrows); (J-L) MR T2 axial, T1 sagittal and coronal images of a 3-month-old patient with pontocerebellar hypoplasia 6 (*RARS2* mutation) showing pontocerebellar hypoplasia with butterfly appearance on coronal images (white arrows).

 

**Table 1** The main imaging features of the pontocerebellar hypoplasia subtypes are reported

| Subtype | Brainstem and cerebellum | Cerebral hemispheres | Others MRI and clinical findings |
|---|---|---|---|
| PCH1 | Variable degree of ponto-cerebellar atrophy; in EXOSC3 mutation both dragonfly and butterfly appearance have been described; the dragonfly pattern is the most frequent | Progressive atrophy not present at birth; the rate of progression is linked to the gene defect; atrophy of caudate nuclei | Hypoplastic corpus callosum (EXOSC8); motor neuron degeneration in anterior horn of spinal cord; optic atrophy |
| PCH2 | PCH2A (pTSEN54 mutation), PCH2B (TSEN2), PCH2C (TSEN34) and PCH2F (TSEN15): dragonfly appearance; PCH2B, PCH2C and PCH2F the ponto-cerebellar atrophy is less severe; PCH2D (SEPSECs mutation): butterfly appearance; pontine atrophy can be absent; PCH2E (VPS53 mutation): cerebellar atrophy is absent at birth and develops during first year of life | Progressive atrophy absent in neonatal period | Corpus callosum is hypoplastic; optic atrophy (PCH2D) |
| PCH3 | Homozygous mutation in the *PCLO* gene causing synaptic dysfunction and apoptosis, hence resulting in neuronal loss; ponto-cerebellar hypoplasia; pons and cerebellum equally affected | Progressive atrophy present at birth | Corpus callosum is thin; optic atrophy |
| PCH4 | Homozygous or compound heterozygous mutation in the *TSEN54* gene; butterfly appearance; atrophy is rapid and severe; C-shaped olivari nuclei; hypoplastic dentate nuclei | Rapid and severe atrophy; caudate nuclei and thalami atrophy | – |
| PCH5 | Compound heterozygous mutation in the *TSEN54* gene; ponto-cerebellar atrophy is rapid and severe; C-shaped olivari nuclei, hypoplastic dentate nuclei | Diffuse atrophy | – |
| PCH6 | RARS2 mutation; rapidly progressive and severe atrophy that may be absent when symptoms starts; pons may be preserved | Marked progressive atrophy, more evident than infratentorial atrophy | – |
| PCH7 | Homozygous or compound heterozygous mutation in the *TOE1* gene; ponto-cerebellar atrophy with sparing of vermis; inferior olivari nuclei and ventral pontine nuclei are absent | Progressive atrophy | Corpus callosum is thin; sex development disorder |
| PCH8 | Homozygous mutation in the *CHMP1A* gene; profound hypoplasia with dragonfly appearance but no evidence of disease progression | Mild atrophy | Corpus callosum is thin |
| PCH9 | Homozygous mutation in the *AMPD2* gene; dragonfly appearance; a figure of "8" midbrain in axial images | Cerebral white matter loss with periventricular leukomalacia | Corpus callosum is thin or absent |
| PCH10 | Homozygous mutation in the *CLP1* gene; mild cerebellar atrophy (vermis and hemispheres) | Prominent temporal pole atrophy; simplified gyral pattern | Corpus callosum is thin; vertical clivus |
| PCH11 | Homozygous mutation in the *TBC1D23* gene; non progressive moderate to severe ponto-cerebellar hypoplasia | Normal or mild hypoplasia | Corpus callosum is hypoplastic or absent |

hemispheres and a butterfly type where hemispheres and vermis are both reduced in size to a similar extent. A typical example of dragonfly patterns is PCH2A due to *TSEN54* mutation (6-8). On the other hand, PCH8 patients show profound PCH with a dragonfly appearance and no evidence of disease progression (7). In PCH1, due to *EXOSC3* mutation, both dragonfly and butterfly patterns of cerebellar hemisphere involvement have been described, with the dragonfly pattern being the most frequent (9).

We have summarized the most relevant imaging features of the PCH subtypes in *Table 1*.

### *Specific MRI patterns*

❖ CASK-related disorders, due to mutations or deletions of the CASK gene, are characterized by microcephaly

 

and butterfly PCH, possible asymmetry of cerebellar hemispheres and preserved corpus callosum may be present (apart from PCH9) (10). These patients are predominantly females.

- Other dragonfly PCHs are PCH2D, caused by *SEPSECs* mutation (11), and PCH4. Additionally in PCH4 MRI shows C-shaped inferior cerebellar olives, due to their lack of folding, this is the reason why the disease was also known as olivoPCH (12). Moreover in PCH2D pontine hypoplasia can be absent (11) (i.e., only dragonfly cerebellum).
- Extreme thinning or even dysgenesis of corpus callosum may be present (together with PCH9) in PCH8, PCH1 subtype caused by *EXOSC8* mutation, PCH2D, PCH10 and PCH11 (2,4,7,11,12). Thus, the size of corpus callous may range from normal (i.e., CASK) to very atrophic, and needs to be always evaluated when the suspect of PCH arises on images.
- Cortical malformation associated with marked vermian atrophy are described in PCHs due to mutations in *RELN* and *VLDLR* genes (7). Moreover in CASK-related disorders neocortical malformations, with a reduced gyral pattern, can also be observed (10).
- Diffuse T2/FLAIR hyperintensity of the cerebellar cortex in the context of PCH can suggest the diagnosis of congenital disorders of glycosylation type 1a (CDG-1a) (13), although this is not a very specific finding in our experience as it is described also in other mitochondrial diseases (coenzyme Q10 deficiency and complex I deficiency due to NUBPL mutations) and other neurodegenerative diseases (infantile neuroaxonal dystrophy and late infantile neuronal ceroid lipofuscinosis) (14).
- Evolution of the atrophy: cerebral atrophy can be present at birth, as in PCH3, or can occur later and progress over time, as in PCH1, PCH2, PCH6, and PCH7 (7,9,11,15). As a result, each PCH subtype has a highly variable disease course. For instance, the progression of symptoms and of atrophy, is more rapid and severe in PCH4, PCH5 and PCH6 whereas in PCH8 and PCH11 there is no evidence of disease progression (7). The term PCH can be misleading as it suggests a static process. Nevertheless, the PCH group includes non-progressive diseases (types 3 and 8) as well as prenatal onset degenerative disorders (types 1, 2, 4, 5, 6, and 7) (7) in which the term atrophy would be more appropriate.
- Ophthalmology complications in PCH may relate to optic atrophy, which is well described in PCH1 (16) as well as in PCH2D, PCH3 and CASK-related disorders (7,10,12).
- Measurements are more useful in cases of suspected hypoplastic cerebellum than in atrophy cases. Most of the normal values available in literatures refers to ratio with the supratentorial brain and seem to be also useful in evaluation of cerebellar enlargement (macrocerebellum) (17).
- Pseudo-PVL pattern can be found in patients with PCH7 as a marked reduction in the white matter bulk with severe ventriculomegaly. This pseudo-PVL pattern is usually associated with corpus callosum anomalies, and an equal involvement of vermis and hemispheres although with a higher degree of hypoplasia and atrophy (7). However, clinical features are strikingly different and the radiological features can help formulating this differential diagnosis.

## Conclusions

PCH9 has typical imaging findings characterized by dragonfly cerebellar atrophy, PVL, extreme thinning of the corpus callosum and abnormal midbrain describing a figure of "8" in axial images. This constellation of findings may be considered pathognomonic and can be used to differentiate PCH9 from other PCH subtypes.

## Acknowledgments

None.

## Footnote

*Conflicts of Interest:* The authors have no conflicts of interest to declare.

## References

1. Marsh APL, Novarino G, Lockhart PJ, Leventer RJ. CUGC for pontocerebellar hypoplasia type 9 and spastic paraplegia-63. Eur J Hum Genet 2019;27:161-6.
2. Marsh APL, Lukic V, Pope K, Bromhead C, Tankard R, Ryan MM, Yiu EM, Sim JC, Delatycki MB, Amor DJ, McGillivray G, Sherr EH, Bahlo M, Leventer RJ, Lockhart PJ. Complete callosal agenesis, pontocerebellar hypoplasia, and axonal neuropathy due to AMPD2 loss. Neurol Genet 2015;16;1:e16.
3. Accogli A, Iacomino M, Pinto F, Orsini A, Vari MS, Selmi R, Torella A, Nigro V, Minetti C, Severino M, Striano P, Capra V, Zara F. Novel AMPD2 mutation in

 

pontocerebellar hypoplasia, dysmorphisms, and teeth abnormalities. Neurol Genet 2017;3:e179.
4. Akizu N, Cantagrel V, Schroth J, Cai N, Vaux K, McCloskey D, Naviaux RK, Van Vleet J, Fenstermaker AG, Silhavy JL, Scheliga JS, Toyama K, Morisaki H, Sonmez FM, Celep F, Oraby A, Zaki MS, Al-Baradie R, Faqeih EA, Saleh MA, Spencer E, Rosti RO, Scott E, Nickerson E, Gabriel S, Morisaki T, Holmes EW, Gleeson JG. AMPD2 regulates GTP synthesis and is mutated in a potentially treatable neurodegenerative brainstem disorder. Cell 2013;154:505-17.
5. Marsh APL, Yap P, Tan T, Pope K, White SM, Chong B, Mcgillivray G, Boys A, Stephenson SE, Leventer RJ, Stark Z, Lockhart PJ. A novel AMPD2 mutation outside the AMP deaminase domain causes pontocerebellar hypoplasia type 9. Am J Med Genet A 2017;173:820-23.
6. Namavar Y, Barth PG, Kasher PR, van Ruissen F, Brockmann K, Bernert G, Writzl K, Ventura K, Cheng EY, Ferriero DM, Basel-Vanagaite L, Eggens VR, Krägeloh-Mann I, De Meirleir L, King M, Graham JM Jr, von Moers A, Knoers N, Sztriha L, Korinthenberg R; PCH Consortium, Dobyns WB, Baas F, Poll-The BT. Clinical, neuroradiological and genetic findings in pontocerebellar hypoplasia. Brain 2011;134:143-56.
7. van Dijk T, Baas F, Barth PG, Poll-The BT. What's new in pontocerebellar hypoplasia? An update on genes and subtypes. Orphanet J Rare Dis 2018;13:92.
8. Feinstein M, Flusser H, Lerman-Sagie T, Ben-Zeev B, Lev D, Agamy O, Cohen I, Kadir R, Sivan S, Leshinsky-Silver E, Markus B, Birk OS. VPS53 mutations cause progressive cerebello-cerebral atrophy type 2 [PCCA2]. J Med Genet 2014;51:303-8.
9. Eggens VR, Barth PG, Niermeijer JMF, Berg JN, Darin N, Dixit A, Fluss J, Foulds N, Fowler D, Hortobágyi T, Jacques T, King MD, Makrythanasis P, Máté A, Nicoll JA, O'Rourke D, Price S, Williams AN, Wilson L, Suri M, Sztriha L, Dijns-de Wissel MB, van Meegen MT, van Ruissen F, Aronica E, Troost D, Majoie CB, Marquering HA, Poll-Thé BT, Baas F. EXOSC3 mutations in pontocerebellar hypoplasia type 1: novel mutations and genotype-phenotype correlations. Orphanet J Rare Dis 2014;9:23.
10. Burglen L, Chantot-Bastaraud S, Garel C, Milh M, Touraine R, Zanni G, Petit F, Afenjar A, Goizet C, Barresi S, Coussement A, Ioos C, Lazaro L, Joriot S, Desguerre I, Lacombe D, des Portes V, Bertini E, Siffroi JP, de Villemeur TB, Rodriguez D. Spectrum of pontocerebellar hypoplasia in 13 girls and boys with CASK mutations: confirmation of a recognizable phenotype and first description of a male mosaic patient. Orphanet J Rare Dis 2012;7:18.
11. Pavlidou E, Salpietro V, Phadke R, Hargreaves IP, Batten L, McElreavy K, Pitt M, Mankad K, Wilson C, Cutrupi MC, Ruggieri M, McCormick D, Saggar A, Kinali M. Pontocerebellar hypoplasia type 2D and optic nerve atrophy further expand the spectrum associated with selenoprotein biosynthesis deficiency. Eur J Paediatr Neurol 2016;20:483-8.
12. Namavar Y, Barth PG, Poll-The BT, Baas F. Classification, diagnosis and potential mechanisms in pontocerebellar hypoplasia. Orphanet J Rare Dis 2011;6:50.
13. Feraco P, Mirabelli-Badenier M, Severino M, Alpigiani MG, Di Rocco M, Biancheri R, Rossi A. The shrunken, bright cerebellum: a characteristic MRI finding in congenital disorders of glycosylation type 1a. AJNR Am J Neuroradiol 2012;33:2062-7.
14. Anderson C, Davies JH, Lamont L, Foulds N. Early pontocerebellar hypoplasia with vanishing testes: A new syndrome? Am J Med Genet A 2011;155A:667-72.
15. Ivanov I, Atkinson D, Litvinenko I, Angelova L, Andonova S, Mumdjiev H, Pacheva I, Panova M, Yordanova R, Belovejdov V, Petrova A, Bosheva M, Shmilev T, Savov A, Jordanova A. Pontocerebellar hypoplasia type 1 for the neuropediatrician: Genotype-phenotype correlations and diagnostic guidelines based on new cases and overview of the literature. Eur J Paediatr Neurol 2018;22:674-81.
16. D'Arco F, Ugga L, Caranci F, Riccio MP, Figliuolo C, Mankad K, D'Amico A. Quant Imaging Med Surg 2016;6:496-503.
17. Poretti A, Wolf NI, Boltshauser E. Differential diagnosis of cerebellar atrophy in childhood. Eur J Paediatr Neurol 2008;12:155-67.

**Cite this article as:** Scola E, Ganau M, Robinson R, Cleary M, De Cocker LJ, Mankad K, Triulzi F, D'Arco F. Neuroradiological findings in three cases of pontocerebellar hypoplasia type 9 due to *AMPD2* mutation: typical MRI appearances and pearls for differential diagnosis. Quant Imaging Med Surg 2019;9(12):1966-1972. doi: 10.21037/qims.2019.08.12

 